The Expression of Interleukin-1β is Regulated by DNA Methylation in Microglia to Mediate Postoperative Cognitive Dysfunction in Aged Mice

Yin Gao
Xuzhou Medical University
Li Yang
Xuzhou Medical University
Xiu Yang
Xuzhou Medical University
Jing-Ru Hao
Xuzhou Medical University
Xiao-Ran Shen
Xuzhou Medical University
Hu-Yi Wang
Xuzhou Medical University
Xu Li
Xuzhou Medical University
Yue-Ying Liu
Xuzhou Medical University
Le Liu
Xuzhou Medical University
Kun Tong
Xuzhou Medical University
Yue You
Xuzhou Medical University
Di-Shi Chen
Xuzhou medical university
Nan Sun
Xuzhou Medical University
Can Gao (gaocan@xzhmu.edu.cn)
Xuzhou Medical University https://orcid.org/0000-0001-5552-9639

Research Article

Keywords: DNA methylation, IL-1β, Microglia, POCD, Synaptic plasticity

Posted Date: October 27th, 2021

DOI: https://doi.org/10.21203/rs.3.rs-973050/v1

Abstract

Postoperative cognitive dysfunction (POCD) is a common postoperative complication in elderly individuals. Neuroinflammation is closely related to its occurrence. However, the exact molecular mechanism underlying this link is undetermined. This study aimed to establish a mouse model of POCD to explore the role of DNA methylation in regulating the expression of interleukin-1β (IL-1β), which mediates the occurrence of POCD in aged mice. The POCD model was established by exploratory laparotomy and evaluated by novel object and Y-maze tests. We also assessed IL-1β production in the dorsal hippocampus and the expression of the DNA methylation-related proteins DNA methyltransferase 3a (DNMT3a), DNA methyltransferase 3b (DNMT3b), and methyl CpG binding protein 2 (MeCP2). Methylation specific PCR (MSP), methylated DNA immunoprecipitation (MeDIP) and DNA methylation sequencing in IL-1β promoter were used to explore the regulation of IL-1β by DNA methylation in this model. Finally, Golgi-Cox staining and Western blotting were used to further explore the role and potential mechanisms of IL-1β in POCD. Cognitive impairment was observed in aged but not adult mice. In aged mice, the microglia cells in the dorsal hippocampus were activated, while the DNA methylation in the IL-1β promoter was decreased. Interestingly, the global DNA methylation in the dorsal hippocampus was unchanged. IL-1β inhibition prevented surgery-induced cognitive decline and dysfunction of synaptic plasticity. Overall, these results indicated that DNA methylation regulation of IL-1β expression may be an important mechanism increasing the susceptibility to POCD.

Introduction

Postoperative cognitive dysfunction (POCD) is a clinical phenomenon that is characterized by disturbances in memory, intellectual ability and executive function which adversely affects quality of life, social dependence and mortality [1]. The incidence of POCD in middle-aged patients is 19.2% [2] and up to 52% in aged patients [3, 4]. Increased susceptibility to POCD has also been found in aged animals [5–8]. However, the molecular mechanism for the high incidence of this complication in elderly individuals remains controversial.

During aging, excessive release of interleukin-1β (IL-1β) and microglial priming are usually considered the main causes of POCD, as IL-1β and microglia are at the nexus of crosstalk between neuroinflammation and abnormal neuronal function and synaptic injury [9, 10]. IL-1β, IL-1β receptors and the naturally occurring interleukin-1 receptor antagonist (IL-1ra) are expressed at comparatively high levels in the hippocampus, a brain structure critical for spatial and contextual memory [11, 12]. However, the mechanisms by which anesthesia and surgery cause excessive release of IL-1β in elderly individuals and by which aberrantly elevated levels of IL-1β in the hippocampus may impair synaptic plasticity and memory are unclear.

It’s established that epigenetic regulation plays a key role in inflammatory and cognitive behavioral changes. DNA methylation is a reversible epigenetic mechanism associated with gene silencing [13, 14]. This modification is catalyzed by DNA methyltransferases (DNMTs), including DNMT1, DNMT3a, and

DNMT3b. Another protein associated with DNA methylation is methyl CpG binding protein 2 (MeCP2), which binds to methylated cytosine bases and recruits histone deacetylases and other corepressors [15]. Clinical trials showed that postoperative global hypomethylation of leukocyte DNA was associated with the development of early POCD [16]. Furthermore, functional genomic analysis revealed that the mRNA expression profiles of various genes involved in the neuroinflammatory response in the brains of subjects with late-onset Alzheimer's disease. It was only IL-1β that showed a pattern compatible with the expected "low DNA methylation / high mRNA expression" relationship [17]. In addition, a novel finding indicated that aged mice exhibited decreased methylation of the IL-1β gene promoter in microglia following systemic LPS administration, an effect that is associated with increased IL-1β mRNA transcription and intracellular IL-1β production, as well as prolonged sickness behavior [18]. Although DNA methylation was involved in multiple aspects of IL-1β and memory, the mechanism by which DNA methylation and IL-1β mediated POCD remains unclear.

In the present study, we investigated the role of DNA methylation in the regulation of IL-1β expression and the occurrence of POCD. Our study demonstrated that surgery impaired memory formation in aged but not in adult mice, an effect that was correlated with decreased levels of DNA methylation in microglia, increased expression of IL-1β, decreased expression of DNMT3a, DNMT3b and MeCP2 in the dorsal hippocampus. In addition, suppression of IL-1β expression in the dorsal hippocampus prevented surgery-induced dysfunction of synaptic plasticity and cognitive decline in aged mice.

Materials And Methods

Animals

Male C57BL/6J mice (3-month-old (3 m) mice weighing 21-25 g and 18 month-old (18 m) mice weighing 28-32 g) were obtained from the animal center of Xuzhou Medical University. The animals were acclimatized for 7 days before the experiments and were housed in groups with the same cage mates throughout the acclimation and experimental periods. All mice were housed under standard conditions with five mice per cage in a room (22-25°C, 40-60% humidity) maintained on a 12 h/12 h dark/light cycle with access to food and water ad libitum.

Mouse model of POCD

An exploratory laparotomy was performed under isoflurane (RWD Life Science, 20052802, China) anesthesia to establish the POCD model, as described in other studies [19, 20]. The 3 m and 18 m mice were randomly divided into five groups: sham group, isoflurane (Iso) group, 1 day after surgery (1d) group, 3 days after surgery (3d) group, and 7 days after surgery (7d) group. Mice in the sham group remained in a chamber filled with 100% oxygen and were not subjected to any anesthesia/surgical procedure. Mice in the Iso group were anesthetized with 5% isoflurane for induction followed by 1.4-2% isoflurane for maintenance for 20 min without being subjected to any surgical procedure. Mice in the surgery groups were anesthetized with 5% isoflurane for induction followed by 1.4-2% isoflurane for maintenance. Next, a longitudinal midline incision (approximately 1 cm) was made for entry into the

abdominal cavity through the skin, abdominal muscles, and peritoneum. Then, a 5-cm segment of the small intestine was pulled out of the abdominal cavity and gently massaged for 30 s. Finally, sterile 4-0 chromic gut sutures were used to suture the incision layer by layer. The operation time for each mouse was approximately 20 min, during which the body temperature of the mouse was monitored and kept between 36°C and 37°C by a heating pad. Simultaneously, the operator monitored the concentration of isoflurane and flow of oxygen, maintaining a pinkish hue in the mouth, nose, and limbs of the mouse and a breathing rate of 70-80 breaths/min. After the mice recovered from anesthesia/surgery, they were returned to their home cages. Compound lidocaine cream (2.5% lidocaine and 2.5% prilocaine) was applied locally to treat postoperative pain.

Open field test (OFT)

An open field apparatus consisting of a black Plexiglas chamber with a white floor (35 cm × 23 cm × 23 cm) was positioned in a dimly lit room. The OFT was used to measure the locomotor activity of the mice at different time points, as we described previously [20]. In brief, mice were placed individually into the center of the apparatus and were allowed to freely explore the environment for 5 min. The total distance traveled by the mouse was automatically recorded with ANY-maze software (ANY-maze, Stoelting Co., IL, USA). The apparatus was wiped with 75% ethanol after each test to avoid olfactory cues (animal scent, stool, urine, etc.).

Object location memory (OLM) and object recognition memory (ORM) tasks

The novel object test apparatus was adjusted according to the method described by Annie Vogel-Ciernia [21–26]. The novel object test was performed using a 35 × 23-cm open arena with 23-cm-high walls. For habituation, a researcher transported the mouse to the chamber and lowered it to the bottom. Then, the researcher gently turned his or her hand so that the mouse could step out of his or her hand into the chamber and allowed the mouse to explore freely for 30 min. During the training session, the mouse was exposed to two familiar objects and allowed to explore them for 15 min. Then, the mouse was returned to its cage. For the OLM task, one of the two familiar objects was moved to a new location 2 hours after the training session. For the ORM task, the object locations remained constant, but one of the objects was replaced with a new item. After the object was exchanged, the mouse was allowed to freely explore the area for 10 min. An exploration was scored when the mouse oriented its head toward the object and came within 1 cm or when the nose of the mouse touched the object. Preference for the novel item was expressed as a discrimination index (DI) = (t novel -t familiar) / (t novel + t familiar). Mice that explored both objects for less than 2 s during testing or 3 s during training were excluded from further analysis. Mice that showed a preference for one object during training (DI > ± 0.2) were also excluded.

Y-maze test

The Y-maze consisted of three opaque arms (8 × 30 × 15 cm, width × length × height) oriented 120° with respect to each other. Mice were handled for 2 min/day for 4 days. For the spatial reference memory test, the mouse was allowed to explore the maze with the novel arm blocked for 15 min during training. After a

2-h interval, the mouse was placed back into the maze with the block removed, and the time spent in the novel arm was recorded. For the spontaneous alternation test, the mouse was allowed to explore the maze for 15 min during training. After a 2-h interval, the mouse was allowed to explore the maze undisturbed for 8 min, and the numbers of all arm entries and alternations were simultaneously recorded. An alternation was defined as a consecutive entry into all three arms. The alternation percent (%) was calculated using the following formula: alternation % = number of alternations / (total number of arm entries – 2) × 100 [27].

Western blot analysis

Western blotting was performed as we described previously [28]. In brief, total protein and nuclear protein were extracted with radioimmunoprecipitation assay (RIPA) buffer (Beyotime, P0013B, China) containing protease inhibitor cocktail (Glpbio, GK10014, USA). Then, the nuclear protein were extracted with ProteoExtract® Subcellular Proteome Extraction Kit (Millipore, 539790, Germany). SDS-PAGE was used to separate the proteins, which were subsequently transferred to polyvinylidene fluoride (PVDF) membranes (GE Healthcare, A29562259, USA). Membranes were incubated with the following primary antibodies: anti-NF-κB P65 (1:1000; Cell Signaling, 8242P; USA), anti-Iba1 (1:1000; Abcam, ab178846; UK), anti-GFAP (1:1000; Abcam, ab53554; UK), anti-PSD95 (1:1000; Sigma, p246; USA), anti-Synaptophysin (1:1000; 5461S; Cell Signaling, USA), anti-BDNF (1:1000; ab108319; Abcam, UK), anti-DNMT3a (1:1000; Cell Signaling, 2160S; USA), anti-DNMT3b (1:1000; Abcam, ab2851; UK), anti-MeCP2 (1:1000; Cell Signaling, 3456T; USA), anti-PCNA (1:1000; Abcam, ab2426; UK), anti-GAPDH (1:1000; Proteintech, 10494-1; USA) and anti-β-actin (1:1000; Bioss, bsm-33036M; China) at 4°C overnight. Membranes were incubated with HRP-conjugated secondary antibodies (1:1000; Beyotime, China) and developed with an ECL detection system (Beyotime). ImageJ software was used to quantify protein band densities.

Enzyme-linked immunosorbent assay (ELISA)

Dorsal hippocampal homogenate was obtained on days 1, 3, and 7 after surgery and day 1 after isoflurane anesthesia. The homogenate was centrifuged at 12000 × g and 4°C for 15 min to collect the supernatant. IL-1β (ABclonal, RK00006, USA) was measured according to the manufacturer's protocols. The optical density (OD) values at 450 nm and 630 nm were measured with an ELISA plate reader (Multiskan GO, Thermo Fish Scientific, USA).

Quantitative real-time reverse transcription PCR (RT-PCR)

Total RNA was extracted from the dorsal hippocampus using a TaKaRa MiniBEST Universal RNA Extraction Kit (TaKaRa, 9767, China) according to the manufacturer's protocol. cDNA was synthesized from 500 ng of RNA with PrimeScript ™ RT Master Mix (Perfect Real Time) (TaKaRa, RR036A, China), and real-time RT-PCR was performed in triplicate according to the protocol of the TB Green® Premix Ex Taq™ (Tli RNaseH Plus) Kit (TaKaRa, RR420A, China) with the following primers: IL-1β, F: 5'-CCTTGTGCAAGTGTCTGAAG-3' and R: 5'-GGGCTTGGAAGCAATCCTTA-3'; DNMT3a, F: 5'-CTGGTGATTGGAGGCAGTCCATGCA-3' and R: 5'-TAGCTGAGGCTGTCTGCATCGGACA-3'; DNMT3b, F: 5'-GGATGTTCGAGAATGTTGTGGCC-3' and R: 5'-CAGGTCAGACCTCTCTGGTGACAAG-3'; MeCP2, F: 5'-

GGTAAAACCCGTCCGGAAAATG-3' and R: 5'-TTCAGTGGCTTGTCTCTGAG-3'; GAPDH, F: 5'-TGAAGGTCGGAGTCAACGGATTTGGT-3' and R: 5'-CATGTGGGCCATGAGGTCCACCAC-3'. The relative expression level of each target gene was determined by the $2^{-\Delta\Delta CT}$ method and expressed as the fold change compared with a control.

Immunofluorescence staining

Mice were perfused transcardially via the left ventricle with 0.9% saline followed by 4% paraformaldehyde in 0.1 M phosphate buffer (pH 7.4). Brain tissues were harvested, postfixed with 4% paraformaldehyde overnight and dehydrated in 30% sucrose, as we reported previously [29]. Sections (35 μm thick) were sliced with a freezing microtome (Leica CM1950, Germany). The brain tissue was blocked with 10% normal donkey serum in phosphate-buffered saline supplemented with Tween 20 (PBST) for 1 h at room temperature and was then incubated with primary antibodies against Iba1 (1:200; 019-19741; FUJIFILM Wako Pure Chemical Corporation, Japan), GFAP (1:200; 3670S; Cell Signaling, USA), c-Fos (1:200; 226003; SYSY, Germany), and Neuronal Nuclei (1:200; MAB377; Millipore, USA) in a cold room at 4°C overnight. The brain tissue was then incubated with donkey anti-rabbit Alexa Fluor 594 (1:400; A21207; Invitrogen, USA) and donkey anti-mouse Alexa Fluor 488 (1:400; A32766; Invitrogen, USA) as the secondary antibodies at room temperature in the dark for 2 h. Then, the sections were mounted with DAPI Fluoromount-G (Southern Biotech, USA). The fluorescence was visualized under an FV-1000 confocal fluorescence microscope (Olympus, Japan). For each animal, the fluorescence intensities from three slides (three visual fields per slide) were averaged [30].

Golgi-Cox staining and dendritic spine counting

Golgi-Cox impregnation is an effective method for studying the morphology of neurons and visualizing structural synaptic plasticity [31]. An FD Rapid GolgiStain^{TM} Kit (FD Neurotechnologies, PK401, Columbia) was employed according to the manufacturer's instructions. In brief, mice were deeply anesthetized by isoflurane and rapidly sacrificed. The brains were removed as quickly as possible, washed with double-distilled water, immersed in impregnation solution (a mixture of solutions A and B), and stored in the dark at room temperature for 14 days. Next, the samples were transferred to solution C and stored at 4°C in the dark for at least 72 h. Finally, the brains were sliced at a thickness of 150 μm with an oscillating tissue slicer (chamber temperature -22°C), stained and mounted on gelatin-coated slides. After alcohol dehydration, the tissue sections were cleared in xylene and coverslipped. The dendrites from hippocampal neurons in the CA1 region were imaged with a confocal microscope (100× oil objective). The dendritic spine density was determined along CA1 secondary dendrites starting from their point of origin on the primary dendrite, and counting in each sample was performed by an experimenter blinded to the group allocation.

Dot blot analysis

Total DNA (250 ng, 3 μl) was diluted with incubation buffer (65.7% ammonium acetate, 7.77% formaldehyde (37-40%), and 6.8% MOPS) to 9 μl and incubated at 65°C for 5 min. Then, 12 μl of 20× saline-sodium citrate was added. The above mixture (5 μl) was spotted onto a Hybond-N^+ membrane (GE

Amersham, RPN303B, UK). DNA was hybridized to the membrane by a 10 min incubation with UV crosslinking. Then, the membrane was immersed in a solution of methylene blue and mixed liquor (0.02% methylene blue and 0.3 M sodium acetate) for 5-10 min. The membrane was then incubated with a 1:1000 dilution of an anti-5-methylcytosine (5mC) antibody (Active Motif, 61255, USA) at 4°C overnight. After three rounds of washes with 1× PBST, the membrane was incubated with the corresponding secondary antibody for 2 h. Finally, an ECL detection system (Beyotime) and ImageJ were used for data analysis and statistical calculations [32].

Cell culture and treatment, lentivirus production and lentiviral transduction

For culture of BV2 microglia and HEK293T cells, the medium was changed every other day using a 1:1 mixture of fresh DMEM (Gibco, RNBJ5984, USA) containing 10% fetal bovine serum (FBS; SE OU Biology, C100-900, China). The cells were incubated at 37°C in a humidified incubator with 5% CO_2 / 95% air and used for experiments after treatment. For lentivirus production and lentiviral transduction, the DNMT3a-green fluorescent protein (GFP) overexpression and empty-GFP plasmids were first constructed by JingMai (Nanjing JingMai Co., Ltd., Nanjing, China). The constructed core plasmid (16 μg) and the packaging and envelope plasmids psPAX2 (12 μg) and pMD2.G (4.8 μg), respectively, were cotransfected into HEK293T cells in a 6-well plate according to the manufacturer's instructions for Lipofectamine 6000 (Beyotime, C0526, China). Then, the supernatant was collected 48 h after transfection and concentrated through a Centricon Plus-70 filter unit (UFC910096, Millipore, USA). Lentivirus with a titer of 10^8 TU/ml was used in the experiment. Lentiviral transduction into BV2 microglia was performed as described in a previous study [33]. In brief, 20 μl of lentiviral solution and 2 μl of polybrene (1.4 μg/μl; H9268, Sigma-Aldrich, USA) were added to a 24-well plate containing 1×10^5 BV2 cells and FBS-free DMEM. After 24 h, the transduction medium was replaced with 500 μl of fresh complete medium containing 10% FBS, and cells were collected 48 h after culture. These cells were divided into four groups: the LPS (-) + Lenti-DNMT3a group, LPS (-) + Lenti-Empty group, LPS (+) + Lenti-DNMT3a group, and LPS (+) + Lenti-Empty group. Cells were treated with LPS (1 μg/ml) or left untreated for 4 h [29].

Microglia isolation

Animals were anesthetized with isoflurane after treatment, and the dorsal hippocampi were harvested on ice and used immediately for microglial isolation via a procedure adapted from Astrid E. Cardona [34]. To ensure that enough cells were recovered, dorsal hippocampi from 2 mice from a given experimental group were pooled. Samples were enzymatically digested using a Papain Dissociation System (Worthington, LK003150, USA). Tissue debris was removed by passing the cell suspension through a 40-mm cell strainer. After myelin removal using 30% Percoll (VICMED, VIC1555, China), cells in PBS supplemented with 0.5% bovine serum albumin (BSA) were incubated for 30 min with an anti-CD11b-APC antibody (5 μl, 17-0112-82, eBioscience, China) and an anti-CD45-FITC antibody (5 μl, 11-0451-82, eBioscience, China) for flow cytometry. The number of isolated $CD11b^+/CD45^{low}$ microglia was approximately 1×10^6 cells per pool of 2 brains and did not differ between the treatment groups.

Methylated DNA immunoprecipitation (MeDIP)

Methylated DNA immunoprecipitation was performed using an anti-5mC antibody (1 μg/reaction, A-1014, Epigentek, USA) as described previously with minor modifications [35, 36]. Genomic DNA was extracted with a TaKaRa MiniBEST Universal Genomic DNA Extraction Kit (TaKaRa, 9765, China), treated with RNase A and quantified using a Nanodrop 2000 spectrophotometer. Then, 50 ng/ml of DNA per sample was prepared using IP buffer (100 mM Tris-HCl (pH 7.40), 150 mM NaCl, and 0.05% Triton X-100) and sonicated (BioruptorTM UCD-200, Diagenode SA, Lige, Belgium) into 200-1000 bp fragments for methylation analysis. The effect of ultrasonication can be seen in more detail in the supplementary information (Supplemental Fig. 1a). Sonicated DNA (2000 ng) was diluted to 150 μl with IP buffer and was then incubated with rotation at 4°C overnight with 2 μl of the anti-5mC antibody and negative control IgG. The next day, the methylated DNA was precipitated with protein G magnetic beads (New England Biolabs, S1430S, USA), washed with IP buffer, extracted with proteinase K in TE buffer with 1% SDS for 2 h at 60°C, and purified with a TaKaRa MiniBEST DNA Fragment Purification Kit (TaKaRa, 9761, Japan). Methylation at selected DNA regions was assayed via quantitative PCR (qPCR) according to the protocol of the TB Green® Premix Ex Taq™ (Tli RNaseH Plus) Kit (TaKaRa, RR420A, China) in a QuantStudio 7 Flex Real-Time PCR System (Thermo Fisher Scientific, USA) with the following thermal cycling program: initial denaturation at 95°C for 1 min; 45 cycles at 95°C for 30 s and 58°C for 20 s; and a final extension step at 72°C for 10 s followed by real-time melt curve analysis to verify product specificity. In addition, agarose gel electrophoresis was used to verify product specificity, and the raw image is shown in supplemental Fig. 1b. The primer sequences were as follows: IL-1β, F: 5'-AGCTCCCTCAGCTTAAGCAC-3' and R: 5'-CACATTCGCAAGTGTGTCAT-3'; GAPDH, F: 5'-AACGACCCCTTCATTGAC-3' and R: 5'-TCCACGACATACTCAGCAC-3'. Ct values for immunoprecipitated samples were normalized to unprocessed (input) DNA. GAPDH, whose expression did not change across the samples, was used as the internal normalization control.

Methylation-specific real-time PCR (MSP)

Sodium bisulfite modification and MSP were used to analyze DNA methylation changes in promoter regions. Bisulfite modification of genomic DNA converts unmethylated cytosine residues into uracil residues. In contrast, methylated cytosine residues remain unconverted. Sodium bisulfite modification of DNA was performed using a CpGenome^{TM} Turbo Bisulfite Modification Kit (Millipore, 2906402, USA) according to the manufacturer's protocol. PCR amplification was carried out according to the instructions of the Episcope MSP Kit (TaKaRa, R100A, China). The primer pairs targeted a methylated and an unmethylated CG dinucleotide in DNA associated with the promoter region of IL-1β or unmethylated β-tubulin-4 as a reference gene, as previously published [37]. The primer sequences were as follows: IL-1β methylated, F: 5'-TTTTAGTTTAAGTATAAGGAGGCGA-3' and R: 5'-ACACATTCGCAAATATATCATCGTA-3'; IL-1β unmethylated, F: 5'-TTTTAGTTTAAGTATAAGGAGGTGA-3' and R: 5'-AACACATTCACAAATATATCATCATA-3'; β-tubulin-4 unmethylated, F: 5'-GGAGAGTAATATGAATGATTTGGTG-3' and R: 5'-CATCTCCAACTTTCCCTAACCTACTTAA-3'. Product specificity was determined by melt curve analysis. For MSP data analysis, the methylation index was

calculated by dividing the fold change value for the methylated primer pair by the fold change value for the unmethylated primer pair as previously described [38, 39].

Intracerebroventricular cannulation and administration of recombinant IL-1ra

IL-1ra functions as a competitive inhibitor of IL-1α and IL-1β, binding to the IL-1 type 1 receptor with an affinity equal to that of IL-1β and without any agonist activity [40]. Administration of IL-1ra directly into the cisterna magna has been reported to effectively block the action of IL-1β within the central nervous system (CNS), including the hippocampus [41]. To confirm the impact of blocking the central action of IL-1β before surgery, 18 m mice were randomly divided into four groups: the sham + vehicle (veh) group, sham + IL-1ra group, 1d + veh group, and 1d + IL-1ra group. An intracerebroventricular cannula was inserted into each mouse as described previously [42, 43]. In brief, mice were anesthetized by intraperitoneal injection of Avertin (isoamyl alcohol, 250 mg/kg) and positioned in a stereotaxic frame so that the plane formed by the frontal and parietal bones was parallel to horizontal zero. A cannula (O.D. 0.41 mm) (RWD Life Science, China) was placed in the left lateral cerebral ventricle according to predetermined coordinates (AP: -0.5 mm; ML: 1.0 mm; DV: -2.1 mm). Mice were allowed to recover for a minimum of 5 days before any further treatment or behavioral test. To verify entry into the lateral cerebral ventricle, 2 μl of clear cerebrospinal fluid (CSF) was drawn and gently pushed back in, and a 3-μl total volume of IL-1ra (4 μg, 480-RM/CF, R&D Systems, Minneapolis, MN) was administered 30 min prior to laparotomy or sham operation. An equal volume of sterile saline was injected into vehicle-treated animals.

Sequenom MassARRAY® methylation analysis of the IL-1β promoter

The detailed procedure was completed by CapitalBio technology, who provided the specific steps. Sequenom's EpiDesigner tool (http://www.epidesigner.com) was used to design primers. Usually, PCR primers should be designed to yield a product within a 200-600 bp range. After the primers were designed, they were synthesized by a biological company. A QIAamp DNA Mini Kit (QIAGEN) and other kits were used to extract DNA from the dorsal hippocampus. The DNA concentration was quantified with a spectrophotometer, and 100 ng of DNA was aliquoted and verified by 0.8% agarose gel electrophoresis. Then, the concentration of qualified DNA was adjusted to 75 ng/μl, transferred to a 384-well plate, and stored at -20°C for later use. The following steps were completed with various types of kits: bisulfite treatment of DNA samples (EZ DNA Methylation-Gold Kit, ZYMO), PCR amplification (PCR Accessory Set, Sequenom), alkaline phosphatase treatment (SAP) (MassCLEAVE Kit, Sequenom), in vitro transcription and RNase digestion (MassCLEAVE Kit, Sequenom), and purification, spotting and mass spectrometry (Spectro CHIP® Arrays and Clean Resin). Refer to the kit instructions for the detailed procedures.

Data analysis and statistical tests

The data are presented as the mean ± SEM values and were analyzed with GraphPad Prism 8.0 (GraphPad Software, Inc.). Statistical comparisons between two groups were made with an independent samples t test. Multiple comparisons were performed with one-way ANOVA followed by the Bonferroni test for multiple comparisons. Differences were considered significant when $P < 0.05$.

Results

Surgery but not anesthesia impaired hippocampus-dependent cognition in aged mice

We first tested whether either surgery or anesthesia alone can affect cognition in aged (18 m) and adult (3 m) mice (Fig. 1a). In the open field test, the total distance traveled did not differ significantly among the groups (aged: F (3, 32) = 1.383, $P = 0.2657$; adult: F (3, 32) = 1.593, $P = 0.2103$, Fig. 1b), meaning that locomotor activity was unaffected. Next, we investigated the effects of surgery on learning and memory. As shown in the novel object test, there was no significant preference in any group during training (Supplemental Fig. 2a, 2b). OLM testing revealed that surgery induced object-place recognition deficits in aged mice 1 day after surgery (F (3, 32) = 7.934, $P = 0.0004$, Fig. 1c). However, ORM was normal (F (3, 32) = 0.7731, $P = 0.5176$, Fig. 1d). Adult mice showed no significant differences among the groups in either OLM (F (3, 32) = 0.9032, $P = 0.4504$, Fig. 1c) or ORM (F (3, 32) = 0.3802, $P = 0.7679$, Fig. 1d). OLM and ORM appear to be dependent on different brain regions. OLM requires the hippocampus for encoding, consolidation, and retrieval [44, 45] and is particularly sensitive to manipulations in the dorsal CA1 region [46], whereas ORM requires the participation of different brain regions, including the perirhinal cortex, insular cortex and medial prefrontal cortex [47, 48]. Therefore, we think that the effect of surgery on the cognitive function of aged mice depends mainly on the dorsal hippocampus. In addition, in the Y-maze test, the spontaneous alternation index (F (3, 32) = 13.07, $P < 0.0001$, Fig. 1e) and the time spent in the novel arm (F (3, 32) = 9.374, $P = 0.0001$, Fig. 1f) were decreased in the 1d group but not in the 3d and 7d groups compared with the sham group for aged mice. In contrast, adult mice showed no significant differences among the groups (F (3, 32) = 0.8422, $P = 0.4809$, Fig. 1e; F (3, 32) = 1.649, $P = 0.1976$, Fig. 1f).

In the present model, anesthesia and surgery often occur concurrently; thus, we explored the effect of isoflurane anesthesia alone on the cognitive function of adult and aged mice. In the OLM task, ORM task, and Y-maze test, the cognitive function of both adult and aged mice did not change compared with that in the control group 1 day after isoflurane anesthesia alone (aged: t = 0.2300, $P = 0.8210$; adult: t = 0.6328, $P = 0.5358$, Fig. 1g; aged: t = 1.088, $P = 0.2926$; adult: t = 0.6767, $P = 0.5083$, Fig. 1h; aged: t = 1.529, $P = 0.1458$; adult: t = 0.3644, $P = 0.7203$, Fig. 1i; aged: t = 0.3268, $P = 0.7481$; adult: t = 1.034, $P = 0.3166$, Fig. 1j). These results suggested that surgical trauma during the perioperative period may play a more important role than anesthesia in POCD. Collectively, these results indicated that surgery induced hippocampus-dependent cognitive decline in aged mice.

Surgery activated microglia in the dorsal hippocampus

Since IL-1β mediates the inflammatory response and affects hippocampal memory function [49], we focused on neuroinflammation induced by IL-1β in the present model. Our data showed that the mRNA expression level of IL-1β ($F(4, 25) = 6.836$, $P = 0.0007$, Fig. 2a) as well as its protein expression level ($F(4, 15) = 7.163$, $P = 0.002$, Fig. 2b) in the dorsal hippocampus were higher in the 1d group than in the sham group in aged mice, while adult mice showed no significant differences among the groups ($F(4, 35) = 0.3623$, $P = 0.8337$, Fig. 2a; $F(4, 15) = 1.558$, $P = 0.2363$, Fig. 2b). Anesthesia alone did not change the IL-1β levels in the 1d group and sham group. Nuclear factor-kappa B (NF-κB) is a transcription factor that plays a crucial role in the expression of proinflammatory cytokines in microglia. After translocation into the nucleus, it upregulates the expression of IL-1β [50]. We next evaluated the nuclear expression level of p65, a subunit of NF-κB, in dorsal hippocampal cells and found that it was increased 1 day after surgery, as expected, in aged mice ($t=5.029$, $P = 0.0125$, Fig. 2c).

IL-1β expression has been documented in neurons, microglia and astrocytes [51–54]. Thus, we assessed the changes in microglia and astrocytes. Immunofluorescence staining showed that ionized calcium binding adapter molecule 1 (Iba1) expression was increased in the CA1 region of the dorsal hippocampus on postoperative day 1 in aged mice ($t = 5.565$, $P = 0.0014$, Fig. 2e). Correspondingly, immunoblotting for Iba1 revealed a visible increase in Iba1 expression in the CA1 region of the dorsal hippocampus of aged mice on postoperative day 1 ($t = 2.537$, $P = 0.0349$, Fig. 2g). More interestingly, the same change was found in adult mice ($t=15.17$, $P < 0.0001$, Fig. 2e, $t = 3.012$, $P = 0.0131$, Fig. 2g). Then, we assessed the changes in astrocytes of adult and aged mice. Neither the glial fibrillary acidic protein (GFAP) area fraction nor the expression of GFAP were significantly different in the 1d group compared with the sham group (aged: $t = 1.486$, $P = 0.1879$; adult: $t = 1.319$, $P = 0.2352$, Fig. 2f; aged: $t = 0.3824$, $P = 0.9241$; adult: $t = 0.4406$, $P = 0.6712$, Fig. 2h). These results demonstrated that microglia but not astrocytes in the dorsal hippocampus were activated after surgery.

Surgery altered epigenetic regulators relevant to DNA methylation in microglia of aged mice

To gain a broader perspective on the role of epigenetic regulators in neuroinflammation, the mRNA and protein expression levels of several enzymes that participate in DNA methylation were measured in the dorsal hippocampus of aged mice 1 day after surgery. No changes were found in the mRNA and protein expression levels of DNMT3a, DNMT3b, and MeCP2 (DNMT3a: $t = 0.001376$, $P = 0.9989$; DNMT3b: $t = 0.1285$, $P = 0.9009$; MeCP2: $t = 1.714$, $P = 0.1248$, Fig. 3a; DNMT3a: $t = 2.019$, $P = 0.0781$; DNMT3b: $t = 1.497$, $P = 0.1728$; MeCP2: $t = 0.1637$, $P = 0.8741$, Fig. 3b).

DNMTs (DNMT3a and DNMT3b) add a methyl group to the 5-carbon of the cytosine ring, particularly in cytosine nucleotides located next to a guanine nucleotide, to form 5mC, a stable repressive regulator of promoter activity [55]. To this end, we assessed the level of 5mC by dot blot analysis. The global 5mC level in the dorsal hippocampus did not significantly differ in the 1d group compared with the sham group ($t = 0.06296$, $P = 0.9528$, Fig. 3c), indicating that the global level of DNA methylation in the dorsal hippocampus remained unchanged. Inflammatory factors are released mainly from microglia. Thus, we

next examined the regulation of gene expression by DNA methylation in microglia. Dorsal hippocampal cells from aged mice after surgery or sham operation were isolated by flow cytometry using anti-CD11b-APC and anti-CD45-FITC antibodies. These cells were identified as $CD11b^{+}/CD45^{low}$ and were thought to be predominantly microglia (Fig. 3d). Then, the mRNA levels of several enzymes that participate in DNA methylation were measured. Notably, the mRNA levels of DNMT3a, DNMT3b and MeCP2 were decreased in aged mice 1 day after surgery (DNMT3a: t = 32.08, $P < 0.0001$; DNMT3b: t = 6.409, $P = 0.0007$; MeCP2: t = 8.632, $P = 0.0001$, Fig. 3e). These results showed that alterations in epigenetic regulators (DNMT3a, DNMT3b and MeCP2) in microglia in the dorsal hippocampus were induced by surgery in aged mice.

Surgery decreased DNA methylation of IL-1β promoter in aged mice

The expression of NF-κB P65 was increased in aged mice 1 day after surgery. Moreover, other studies have reported that NF-κB binding activity might play a role in IL-1β promoter demethylation [56]. Therefore, in this study, we investigated methylation sites adjacent to a canonical NF-κB binding site (CpG sites -229 bp and -215 bp with respect to the translation start site in the IL-1β promoter). As expected, the levels of DNA methylation at the above two sites were reduced by surgery in aged mice (MSP: t = 2.661, $P = 0.0375$; MeDIP: t = 3.753, $P = 0.0095$, Fig. 4a). In contrast, most other CpG sites except for the abovementioned two sites were highly methylated and not affected by surgery; we examined >10 CpG sites in the region between -1439 bp and 760 bp with respect to the ATG translation start codon (Fig. 4b).

To demonstrate whether DNA methylation plays a direct role in IL-1β expression, the BV2 immortalized murine microglial cells were transduced with lentiviral vectors expressing DNMT3a tagged with GFP (Lenti-DNMT3a–GFP) or empty vector (Lenti-Empty-GFP). Then, the cultures were harvested after treatment with LPS. BV2 cells were effectively transduced with Lenti-GFP (Fig. 4c), and the cell morphology did not change. We first detected the expression of DNMT3a, which was significantly reduced by LPS treatment (t = 3.846, $P = 0.0049$, Fig. 4d). After transduction with Lenti-DNMT3a, the expression of DNMT3a was restored compared to that in the Lenti-Empty + LPS (-) group (t = 3.501, $P = 0.0081$, Fig. 4d). Then, we examined the effects of DNMT3a overexpression on IL-1β expression and DNA methylation in the IL-1β promoter. The LPS-induced increase in the expression of IL-1β ($F(3, 12) = 12.00$, $P = 0.0006$, Fig. 4e) and decrease in the DNA methylation in the IL-1β promoter ($F(3, 8) = 10.16$, $P = 0.0042$, Fig. 4f) were reversed by Lenti-DNMT3a transduction. Therefore, these results showed that a decrease in IL-1β promoter DNA methylation was induced by surgery in aged mice. Thus, overexpression of DNMT3a to reverse methylation in the IL-1β promoter could alleviate neuroinflammation induced by LPS.

IL-1β impaired synaptic plasticity after surgery in aged mice

To specifically confirm the role of IL-1β in memory deficits, IL-1ra was injected bilaterally into the lateral cerebral ventricle to suppress the expression of IL-1β in the dorsal hippocampus (Fig. 5a). The level of IL-1β in the dorsal hippocampus of aged mice was reduced by administration of IL-1ra via the lateral

cerebral ventricle just before surgery (F (3, 12) = 11.30, *P* = 0.0008, Fig. 5b). The Golgi-Cox staining results showed that IL-1ra injection reversed the reduction in spine density in the dorsal hippocampal CA1 region (F (3, 12) = 4.841, *P* = 0.0197, Fig. 5d). Regarding synaptic functional plasticity, various genes are related to IL-1β and synaptic function, for example, brain-derived neurotrophic factor (BDNF), postsynaptic density 95 (PSD95), and synaptophysin (Syn), which are involved in learning and memory. The protein expression levels of hippocampal BDNF, PSD95 and syn were significantly decreased in mice in the surgery groups, while IL-1ra injection similarly reversed this change (F (3, 16) = 4.045, *P* = 0.0256, Fig. 5f, F (3, 16) = 4.582, *P* = 0.0169, Fig. 5g, F (3, 12) = 4.877, *P* = 0.0192, Fig. 5h). Furthermore, the number of c-Fos$^+$ neurons in the CA1 region was decreased on postoperative day 1 in aged mice, but IL-1ra injection significantly attenuated the loss of c-Fos$^+$ neurons (F (3, 16) = 17.53, *P* < 0.0001, Fig. 5i). These results indicated that IL-1β impaired synaptic plasticity in the dorsal hippocampus of aged mice in the POCD model.

Inhibiting IL-1β in the dorsal hippocampus rescued memory deficits induced by surgery

Next, we further investigated whether inhibiting IL-1β in the dorsal hippocampus of aged mice by bilateral administration of IL-1ra into the lateral cerebral ventricle rescues the memory deficits induced by surgery. In the open field test, the total distance traveled did not differ significantly among the groups (F (3, 28) = 1.207, *P* = 0.3253, Fig. 6a). In the OLM task, no group showed a significant preference in the novel objection recognition test during training (Supplemental Fig. 2c). During testing, the decrease in the DI was reversed by inhibition of IL-1β (F (3, 28) = 32.07, *P* < 0.0001, Fig. 6b). In the Y-maze test, similarly, in aged mice, the decreases in the spontaneous alternation index and the time spent in the novel arm were reversed by inhibition of IL-1β (F (3, 28) = 10.14, *P* = 0.0001, Fig. 6c; F (3, 28) = 6.361, *P* = 0.0020, Fig. 6d). The above data indicated that the surgery-induced impairment of memory performance was alleviated by suppression of IL-1β.

Discussion

In the present study, we showed that aged mice but not adult mice exhibited hippocampus-dependent postoperative cognitive decline and increased gene expression of IL-1β 1 day after surgery. In aged mice, microglia in the dorsal hippocampus was activated and DNA methylation level of IL-1β promoter was decreased. The increased expression of IL-1β impaired synaptic plasticity and hippocampus-dependent memory formation in aged mice in the POCD model.

However, impairment of OLM and spatial memory did not occur with a single exposure to isoflurane alone in either adult or aged mice, suggesting that a single exposure to isoflurane alone would not induce memory deficits in patients undergoing abdominal surgery. Previous studies have demonstrated that isoflurane exposure in aged rats leads to impaired spatial memory and neuroinflammation [57]. The discrepancies among these studies involving isoflurane inhalation alone might result from the different doses and times. Consistent with this hypothesis, general anesthetics may impair developing neurons

and induce cognitive dysfunction in young adult male C57BL/6 mice in a dose - and time - dependent manner [58, 59]. We also found that the LPS-induced impairment of object recognition and fear memory was not aggravated by isoflurane anesthesia in adult mice [29]. Moreover, Silbert BS et al. found no significant difference in the rate of POCD in a comparison of general anesthesia (containing isoflurane) with spinal anesthesia, suggesting that the surgical or procedural process itself may contribute to the development of POCD [60]. In addition, inflammation increases the sensitivity of neurons to general anesthetics [61].

Accumulating evidence suggests that neuroinflammation and age play critical roles in surgery-induced cognitive impairment [62–64]. Microglia cells are reported to be tuned to different types of host defense and protection depending on the presence of available cytokines. Classical, or “M1,” polarizing signals arm macrophages to elicit the production of proinflammatory and cytotoxic mediators, whereas alternatively activated “M2” macrophages can dampen inflammation and promote tissue regeneration [13, 65, 66]. Other perioperative injury factors, such as reactive oxygen species [67], imbalanced cerebral iron metabolism [68] and downregulated type 2 cannabinoid receptors [69], could also induce microglial activation and ultimately lead to postoperative neurological sequelae. Another important source of IL-1β in the central nervous system (CNS) is astrocytes. The GFAP concentration has been reported to be unrelated to postoperative delirium [70], which is consistent with our results. In addition, astrocytes undergo morphological changes that are not strictly dependent on the GFAP protein level during neuroinflammation [71], Thus, the role of astrocytes in POCD needs to be determined by further experiments.

We demonstrated that age and surgical trauma can alter the expression levels of genes important for establishing and maintaining DNA methylation, such as DNMT3a, DNMT3b and MeCP2 in microglial cells isolated from surgery-treated mice. Interestingly, the global DNA methylation in the dorsal hippocampus was unchanged suggesting that DNA hypomethylation may not be a global phenomenon. In fact, many studies have observed an age-related increase in DNA methylation in the promoters of neuronal activity-related and synaptic marker genes [72, 73] and an age-related decrease in DNA methylation in the promoters of immune-related genes [74]. DNA methylation consistently appears to play a central role in cognitive function and manipulation of DNA methylation-related mechanisms consistently impacts memory processes [75]. The present study suggested that DNA methylation regulated the expression of genes with functions related to neuroinflammation in memory-critical brain regions. However, the mechanism by which DNMTs are targeted to specific genomic sites is unknown. Although studies have suggested that noncoding RNAs [76, 77] or chromatin marks [78, 79] may be responsible for that targeting, these mechanisms are still far from being understood.

The methylation sites investigated in this study are adjacent to a canonical NF-κB-binding site and are individual CpG sites near the transcription start site (TSS). The reason for choosing this site is that IL-1β promoter region in mouse has no CpG island and there is considerable variability in methylation in promoter regions without CpG islands [55]. At the same time, studies have pointed out that several NF-κB (p65/RelA and cRel) consensus sequences have been identified within the Gadd45β gene promoter, and

these sites are involved in the regulation of Gadd45β expression and DNA demethylation in hippocampal neurons during fear memory formation [80]. Evidence in microglia indicates that epigenetic regulation of IL-1β in aged mice could be regulated by increased NF-κB binding, which inhibits proper DNA methylation [56]. Interestingly, Transcriptional regulation of IL-1β through methylation in mouse myeloid cells is very consistent with findings during normal aging in humans and in patients with dementia with tauopathy. One specific CpG site 215 bp upstream of the TSS is found whose methylation status affects the IL-1β transcript level in mouse, which is consistent with our results. Two CpG sites (cg01290568 and cg15836722) are located in the IL-1β gene near the TSS whose methylation negatively correlates with aging and dementia in human [81]. This finding suggests selective regulation of specific CpG sites in the IL-1β gene in both mice and humans could change their cognitive performance. Therefore, our research could provide a new target for the clinical prevention of POCD in elderly individuals.

IL-1β is a key proinflammatory cytokine associated with age-related cognitive decline [82]. IL-1β exerts its biological activity by binding to IL-1 receptor type 1 (IL-1R1). IL-1ra, the endogenous inhibitor of IL-1β, competing with IL-1R1 [40]. Accumulating evidence indicates that synaptic plasticity [83], learning and memory [9] become more vulnerable to IL-1β-mediated impairment. The expression levels of synapse-associated proteins, especially synaptophysin and PSD95, are decreased in the hippocampus of mice treated with LPS. Galantamine not only prevents the LPS-induced reductions in synaptophysin and PSD95 expressions but also increases the dendritic spine density, which can prevent the activation of microglia and improve neuroinflammation by inhibiting inflammatory signaling molecules (NF-κB p65) and cytokines (TNF-α, IL-1β and IL-6) in the hippocampus [84].

Conclusion

In summary, the current study indicated that DNA methylation may be an important mechanism mediating susceptibility to POCD in aged mice by regulating the expression of IL-1β, which could induce synaptic plasticity dysfunction and cognitive decline (Fig. 7). Our results may provide a direction for further research on the relationship among DNA methylation, inflammation and POCD. Our research also provided a new target for the clinical prevention of POCD in elderly individuals.

Declarations

Acknowledgments We are thankful for experimental support from Jiangsu Province Key Laboratory of New Drug Research and Clinical Pharmacy. Financial support from the National Natural Science Foundation of China, the Qing Lan Project of Jiangsu Province, the Natural Science Foundation of Jiangsu Province, and the Postgraduate Research & Practice Innovation Program of Jiangsu Province is also acknowledged. Finally, we also thank Naomi Twery PhD, for polishing the paper.

Author Contributions Can Gao designed and supervised the research; Yin Gao., Li Yang, Xiu Yang, Xu Li, Le Liu, Yue You, Yin Gao, Yue-Ying Liu, Xiao-Ran Shen, Kun Tong, and Di-Shi Chen performed data acquisition, analysis, and interpretation and statistical analysis; Yin Gao and Li Yang wrote the paper; Can

Gao, Yue You, Yin Gao, Yue-Ying Liu, Hu-Yi Wang, Jing-Ru Hao and Nan Sun revised the paper; and Jing-Ru Hao and Nan Sun provided technical and material support. All authors read and approved the final paper.

Funding This work was supported by the National Natural Science Foundation of China (81870852, 82171199), the Qing Lan Project of Jiangsu Province, the Education Department of Jiangsu Province (18KJA320007) and the Natural Science Foundation of Jiangsu Province (BK20181146) to Dr. Gao; the Education Department of Jiangsu Province (17KJB320018) to M.S. Hao; and the Postgraduate Research & Practice Innovation Program of Jiangsu Province (KYCX20_2453 to Dr. X Yang, KYCX20_2454 to Dr. L Yang, and KYCX20_2475 to M.S. Li).

Data Availability The data sets used and analyzed during the current study are available from the corresponding author on reasonable request.

Code Availability Not applicable

Ethics approval and Consent to Participate This study was carried out after approval by the Animal Care and Use Committee of Xuzhou Medical University and in accordance with the Guidelines for the Care and Use of Laboratory Animals and the requirements of the Animal Ethics Committee of Xuzhou Medical University, Jiangsu, China. Extensive efforts were made to ensure minimal suffering of the animals used in the study.

Consent to Participate Not applicable.

Consent for Publication Not applicable.

Competing Interests The authors declare that they have no competing interests.

References

1. Luo A, Yan J, Tang X, Zhao Y, Zhou B, Li S (2019) Postoperative cognitive dysfunction in the aged: the collision of neuroinflammaging with perioperative neuroinflammation. Inflammopharmacology 27(1):27–37. https://doi.org/10.1007/s10787-018-00559-0
2. Johnson T, Monk T, Rasmussen LS, Abildstrom H, Houx P, Korttila K, Kuipers HM, Hanning CD (2002) Postoperative cognitive dysfunction in middle-aged patients. Anesthesiology 96(6):1351–1357. https://doi.org/10.1097/00000542-200206000-000141
3. Monk TG, Weldon BC, Garvan CW, Dede DE, van der Aa MT, Heilman KM, Gravenstein JS (2008) Predictors of cognitive dysfunction after major noncardiac surgery. Anesthesiology 108(1):18–30. https://doi.org/10.1097/01.anes.0000296071.19434.1e
4. Meybohm P, Renner J, Broch O, Caliebe D, Albrecht M, Cremer J, Haake N, Scholz J (2013) Postoperative neurocognitive dysfunction in patients undergoing cardiac surgery after remote

ischemic preconditioning: a double-blind randomized controlled pilot study. PLoS One 8(5):e64743. https://doi.org/10.1371/journal.pone.0064743

5. Li Z, Liu F, Ma H, White PF, Yumul R, Jiang Y, Wang N, Cao X (2017) Age exacerbates surgery-induced cognitive impairment and neuroinflammation in Sprague-Dawley rats: the role of IL-4. Brain Res 1665:65–73. https://doi.org/10.1016/j.brainres.2017.04.004
6. Le Y, Liu S, Peng M, Tan C, Liao Q, Duan K, Ouyang W, Tong J (2014) Aging differentially affects the loss of neuronal dendritic spine, neuroinflammation and memory impairment at rats after surgery. PLoS One 9(9):e106837. https://doi.org/10.1371/journal.pone.0106837
7. Wang Z, Meng S, Cao L, Chen Y, Zuo Z, Peng S (2018) Critical role of NLRP3-caspase-1 pathway in age-dependent isoflurane-induced microglial inflammatory response and cognitive impairment. J Neuroinflammation 15(1):109. https://doi.org/10.1186/s12974-018-1137-1
8. Hovens IB, Schoemaker RG, van der Zee EA, Heineman E, Nyakas C, van Leeuwen BL (2013) Surgery-induced behavioral changes in aged rats. Exp Gerontol 48(11):1204–1211. https://doi.org/10.1016/j.exger.2013.07.011
9. Patterson SL (2015) Immune dysregulation and cognitive vulnerability in the aging brain: Interactions of microglia, IL-1beta, BDNF and synaptic plasticity. Neuropharmacology 96:11–18. https://doi.org/10.1016/j.neuropharm.2014.12.020
10. Salter MW, Stevens B (2017) Microglia emerge as central players in brain disease. Nat Med 23(9):1018–1027. https://doi.org/10.1038/nm.4397
11. Smith DM, Mizumori SJ (2006) Hippocampal place cells, context, and episodic memory. Hippocampus 16(9):716–729. https://doi.org/10.1002/hipo.20208
12. Squire LR, Stark CE, Clark RE (2004) The medial temporal lobe. Annu Rev Neurosci 27:279–306. https://doi.org/10.1146/annurev.neuro.27.070203.144130
13. Petralla S, De Chirico F, Miti A, Tartagni O, Massenzio F, Poeta E, Virgili M, Zuccheri G, Monti B (2021) Epigenetics and Communication Mechanisms in Microglia Activation with a View on Technological Approaches. Biomolecules 11(2):306. https://doi.org/10.3390/biom11020306
14. Cheray M, Joseph B (2018) Epigenetics Control Microglia Plasticity. Front Cell Neurosci 12:243. https://doi.org/10.3389/fncel.2018.00243
15. Dor Y, Cedar H (2018) Principles of DNA methylation and their implications for biology and medicine. Lancet 392(10149):777–786. https://doi.org/10.1016/S0140-6736(18)31268-6
16. Li H, Wu TT, Tang L, Liu Q, Mao XZ, Xu JM, Dai RP (2020) Association of global DNA hypomethylation with post-operative cognitive dysfunction in elderly patients undergoing hip surgery. Acta Anaesthesiol Scand 64(3):354–360. https://doi.org/10.1111/aas.13502
17. Nicolia V, Cavallaro RA, Lopez-Gonzalez I, Maccarrone M, Scarpa S, Ferrer I, Fuso A (2017) DNA Methylation Profiles of Selected Pro-Inflammatory Cytokines in Alzheimer Disease. J Neuropathol Exp Neurol 76(1):27–31. https://doi.org/10.1093/jnen/nlw099
18. Matt SM, Lawson MA, Johnson RW (2016) Aging and peripheral lipopolysaccharide can modulate epigenetic regulators and decrease IL-1beta promoter DNA methylation in microglia. Neurobiol Aging

47:1–9. https://doi.org/10.1016/j.neurobiolaging.2016.07.006

19. Peng M, Zhang C, Dong Y, Zhang Y, Nakazawa H, Kaneki M, Zheng H, Shen Y, Marcantonio ER, Xie Z (2016) Battery of behavioral tests in mice to study postoperative delirium. Sci Rep 6:29874. https://doi.org/10.1038/srep29874
20. Wu T, Sun XY, Yang X, Liu L, Tong K, Gao Y, Hao JR, Cao J, Gao C (2019) Histone H3K9 Trimethylation Downregulates the Expression of Brain-Derived Neurotrophic Factor in the Dorsal Hippocampus and Impairs Memory Formation During Anaesthesia and Surgery. Front Mol Neurosci 12:246. https://doi.org/10.3389/fnmol.2019.00246
21. Holter SM, Garrett L, Einicke J, Sperling B, Dirscherl P, Zimprich A, Fuchs H, Gailus-Durner V, Hrabe de Angelis M, Wurst W (2015) Assessing Cognition in Mice. Curr Protoc Mouse Biol 5(4):331–358. https://doi.org/10.1002/9780470942390.mo150068
22. Sugar J, Moser MB (2019) Episodic memory: Neuronal codes for what, where, and when. Hippocampus 29(12):1190–1205. https://doi.org/10.1002/hipo.23132
23. Vogel-Ciernia A, Wood MA (2014) Examining object location and object recognition memory in mice. Curr Protoc Neurosci 69:8311–8317. https://doi.org/10.1002/0471142301.ns0831s69
24. Lueptow LM (2017) Novel Object Recognition Test for the Investigation of Learning and Memory in Mice. J Vis Exp 126:55718. https://doi.org/10.3791/55718
25. Broadbent NJ, Gaskin S, Squire LR, Clark RE (2010) Object recognition memory and the rodent hippocampus. Learn Mem 17(1):5–11. https://doi.org/10.1101/lm.1650110
26. Leger M, Quiedeville A, Bouet V, Haelewyn B, Boulouard M, Schumann-Bard P, Freret T (2013) Object recognition test in mice. Nat Protoc 8(12):2531–2537. https://doi.org/10.1038/nprot.2013.155
27. Kraeuter AK, Guest PC, Sarnyai Z (2019) The Y-Maze for Assessment of Spatial Working and Reference Memory in Mice. Methods Mol Biol 1916:105-111. https://doi.org/10.1007/978-1-4939-8994-2_10
28. Hao JR, Sun N, Lei L, Li XY, Yao B, Sun K, Hu R, Zhang X, Shi XD, Gao C (2015) L-Stepholidine rescues memory deficit and synaptic plasticity in models of Alzheimer's disease via activating dopamine D1 receptor/PKA signaling pathway. Cell Death Dis 6:e1965. https://doi.org/10.1038/cddis.2015.315
29. Sun XY, Zheng T, Yang X, Liu L, Gao SS, Xu HB, Song YT, Tong K, Yang L, Gao Y, Wu T, Hao JR, Lu C, Ma T, Gao C (2019) HDAC2 hyperexpression alters hippocampal neuronal transcription and microglial activity in neuroinflammation-induced cognitive dysfunction. J Neuroinflammation 16(1):249. https://doi.org/10.1186/s12974-019-1640-z
30. Zhu Y, Wang Y, Yao R, Hao T, Cao J, Huang H, Wang L, Wu Y (2017) Enhanced neuroinflammation mediated by DNA methylation of the glucocorticoid receptor triggers cognitive dysfunction after sevoflurane anesthesia in adult rats subjected to maternal separation during the neonatal period. J Neuroinflammation 14(1):6. https://doi.org/10.1186/s12974-016-0782-5
31. Liu Q, Sun YM, Huang H, Chen C, Wan J, Ma LH, Sun YY, Miao HH, Wu YQ (2021) Sirtuin 3 protects against anesthesia/surgery-induced cognitive decline in aged mice by suppressing hippocampal neuroinflammation. J Neuroinflammation 18(1):41. https://doi.org/10.1186/s12974-021-02089-z

32. Li X, Zhao Q, Wei W, Lin Q, Magnan C, Emami MR, Wearick-Silva LE, Viola TW, Marshall PR, Yin J, Madugalle SU, Wang Z, Nainar S, Vagbo CB, Leighton LJ, Zajaczkowski EL, Ke K, Grassi-Oliveira R, Bjoras M, Baldi PF, Spitale RC, Bredy TW (2019) The DNA modification N6-methyl-2'-deoxyadenosine (m6dA) drives activity-induced gene expression and is required for fear extinction. Nat Neurosci 22(4):534–544. https://doi.org/10.1038/s41593-019-0339-x
33. Pan Z, Li GF, Sun ML, Xie L, Liu D, Zhang Q, Yang XX, Xia S, Liu X, Zhou H, Xue ZY, Zhang M, Hao LY, Zhu LJ, Cao JL (2019) MicroRNA-1224 Splicing CircularRNA-Filip1l in an Ago2-Dependent Manner Regulates Chronic Inflammatory Pain via Targeting Ubr5. J Neurosci 39(11):2125–2143. https://doi.org/10.1523/JNEUROSCI.1631-18.2018
34. Cardona AE, Huang D, Sasse ME, Ransohoff RM (2006) Isolation of murine microglial cells for RNA analysis or flow cytometry. Nat Protoc 1(4):1947–1951. https://doi.org/10.1038/nprot.2006.327
35. Weber M, Davies JJ, Wittig D, Oakeley EJ, Haase M, Lam WL, Schubeler D (2005) Chromosome-wide and promoter-specific analyses identify sites of differential DNA methylation in normal and transformed human cells. Nat Genet 37(8):853–862. https://doi.org/10.1038/ng1598
36. Day JJ, Childs D, Guzman-Karlsson MC, Kibe M, Moulden J, Song E, Tahir A, Sweatt JD (2013) DNA methylation regulates associative reward learning. Nat Neurosci 16(10):1445–1445+. https://doi.org/10.1038/nn.3504
37. Gupta S, Kim SY, Artis S, Molfese DL, Schumacher A, Sweatt JD, Paylor RE, Lubin FD (2010) Histone methylation regulates memory formation. J Neurosci 30(10):3589–3599. https://doi.org/10.1523/JNEUROSCI.3732-09.2010
38. Blaze J, Scheuing L, Roth TL (2013) Differential methylation of genes in the medial prefrontal cortex of developing and adult rats following exposure to maltreatment or nurturing care during infancy. Dev Neurosci 35(4):306–316. https://doi.org/10.1159/000350716
39. Sui L, Wang Y, Ju LH, Chen M (2012) Epigenetic regulation of reelin and brain-derived neurotrophic factor genes in long-term potentiation in rat medial prefrontal cortex. Neurobiol Learn Mem 97(4):425–440. https://doi.org/10.1016/j.nlm.2012.03.007
40. Arend WP, Welgus HG, Thompson RC, Eisenberg SP (1990) Biological properties of recombinant human monocyte-derived interleukin 1 receptor antagonist. J Clin Invest 85(5):1694–1697. https://doi.org/10.1172/JCI114622
41. Barrientos RM, Hein AM, Frank MG, Watkins LR, Maier SF (2012) Intracisternal interleukin-1 receptor antagonist prevents postoperative cognitive decline and neuroinflammatory response in aged rats. J Neurosci 32(42):14641–14648. https://doi.org/10.1523/JNEUROSCI.2173-12.2012
42. Abraham J, Jang S, Godbout JP, Chen J, Kelley KW, Dantzer R, Johnson RW (2008) Aging sensitizes mice to behavioral deficits induced by central HIV-1 gp120. Neurobiol Aging 29(4):614–621. https://doi.org/10.1016/j.neurobiolaging.2006.11.002
43. Abraham J, Johnson RW (2009) Central inhibition of interleukin-1beta ameliorates sickness behavior in aged mice. Brain Behav Immun 23(3):396–401. https://doi.org/10.1016/j.bbi.2008.12.008

44. Cui L, Sun W, Yu M, Li N, Guo L, Gu H, Zhou Y (2016) Disrupted-in-schizophrenia1 (DISC1) L100P mutation alters synaptic transmission and plasticity in the hippocampus and causes recognition memory deficits. Mol Brain 9(1):89. https://doi.org/10.1186/s13041-016-0270-y
45. Haettig J, Stefanko DP, Multani ML, Figueroa DX, McQuown SC, Wood MA (2011) HDAC inhibition modulates hippocampus-dependent long-term memory for object location in a CBP-dependent manner. Learn Mem 18(2):71–79. https://doi.org/10.1101/lm.1986911
46. Vogel-Ciernia A, Matheos DP, Barrett RM, Kramar EA, Azzawi S, Chen Y, Magnan CN, Zeller M (2013) The neuron-specific chromatin regulatory subunit BAF53b is necessary for synaptic plasticity and memory. Nat Neurosci 16(5):552–561. https://doi.org/10.1038/nn.3359
47. Tanimizu T, Kono K, Kida S (2018) Brain networks activated to form object recognition memory. Brain Res Bull 141:27–34. https://doi.org/10.1016/j.brainresbull.2017.05.017
48. Kong Q, Yu M, Zhang M, Wei C, Gu H, Yu S, Sun W, Li N, Zhou Y (2020) Conditional Dnmt3b deletion in hippocampal dCA1 impairs recognition memory. Mol Brain 13(1):42. https://doi.org/10.1186/s13041-020-00574-9
49. Cibelli M, Fidalgo AR, Terrando N, Ma D, Monaco C, Feldmann M, Takata M, Lever IJ, Nanchahal J, Fanselow MS, Maze M (2010) Role of interleukin-1beta in postoperative cognitive dysfunction. Ann Neurol 68(3):360–368. https://doi.org/10.1002/ana.22082
50. Yoshioka Y, Sugino Y, Shibagaki F, Yamamuro A, Ishimaru Y, Maeda S (2020) Dopamine attenuates lipopolysaccharide-induced expression of proinflammatory cytokines by inhibiting the nuclear translocation of NF-kappaB p65 through the formation of dopamine quinone in microglia. Eur J Pharmacol 866:172826. https://doi.org/10.1016/j.ejphar.2019.172826
51. Jones ME, Lebonville CL, Paniccia JE, Balentine ME, Reissner KJ, Lysle DT (2018) Hippocampal interleukin-1 mediates stress-enhanced fear learning: A potential role for astrocyte-derived interleukin-1beta. Brain Behav Immun 67:355–363. https://doi.org/10.1016/j.bbi.2017.09.016
52. Ringwood L, Li L (2008) The involvement of the interleukin-1 receptor-associated kinases (IRAKs) in cellular signaling networks controlling inflammation. Cytokine 42(1):1–7. https://doi.org/10.1016/j.cyto.2007.12.012
53. Huang Y, Smith DE, Ibanez-Sandoval O, Sims JE, Friedman WJ (2011) Neuron-specific effects of interleukin-1beta are mediated by a novel isoform of the IL-1 receptor accessory protein. J Neurosci 31(49):18048–18059. https://doi.org/10.1523/JNEUROSCI.4067-11.2011
54. Liu X, Nemeth DP, McKim DB, Zhu L, DiSabato DJ, Berdysz O, Gorantla G, Oliver B (2019) Cell-Type-Specific Interleukin 1 Receptor 1 Signaling in the Brain Regulates Distinct Neuroimmune Activities. Immunity 50(2):317–333e6. https://doi.org/10.1016/j.immuni.2018.12.012
55. Barter JD, Foster TC (2018) Aging in the Brain: New Roles of Epigenetics in Cognitive Decline. Neuroscientist 24(5):516–525. https://doi.org/10.1177/1073858418780971
56. Schaafsma W, Zhang X, van Zomeren KC, Jacobs S, Georgieva PB, Wolf SA, Kettenmann H, Janova H (2015) Long-lasting pro-inflammatory suppression of microglia by LPS-preconditioning is

mediated by RelB-dependent epigenetic silencing. Brain Behav Immun 48:205–221. https://doi.org/10.1016/j.bbi.2015.03.013

57. Chen L, Xie W, Xie W, Zhuang W, Jiang C, Liu N (2017) Apigenin attenuates isoflurane-induced cognitive dysfunction via epigenetic regulation and neuroinflammation in aged rats. Arch Gerontol Geriatr 73:29–36. https://doi.org/10.1016/j.archger.2017.07.004
58. Liu J, Wang P, Zhang X, Zhang W, Gu G (2014) Effects of different concentration and duration time of isoflurane on acute and long-term neurocognitive function of young adult C57BL/6 mouse. Int J Clin Exp Pathol 7(9):5828–5836
59. Jia M, Liu WX, Yang JJ, Xu N, Xie ZM, Ju LS, Ji MH, Martynyuk AE, Yang JJ (2016) Role of histone acetylation in long-term neurobehavioral effects of neonatal Exposure to sevoflurane in rats. Neurobiol Dis 91:209–220. https://doi.org/10.1016/j.nbd.2016.03.017
60. Silbert BS, Evered LA, Scott DA (2014) Incidence of postoperative cognitive dysfunction after general or spinal anaesthesia for extracorporeal shock wave lithotripsy. Br J Anaesth 113(5):784–791. https://doi.org/10.1093/bja/aeu163
61. Avramescu S, Wang DS, Lecker I, To WT, Penna A, Whissell PD, Mesbah-Oskui L, Horner RL, Orser BA (2016) Inflammation Increases Neuronal Sensitivity to General Anesthetics. Anesthesiology 124(2):417–427. https://doi.org/10.1097/ALN.0000000000000943
62. Kubota K, Suzuki A, Ohde S, Yamada U, Hosaka T, Okuno F, Fujitani I, Koitabashi A, Shimada G, Kishida A (2018) Age is the Most Significantly Associated Risk Factor With the Development of Delirium in Patients Hospitalized for More Than Five Days in Surgical Wards: Retrospective Cohort Study. Ann Surg 267(5):874–877. https://doi.org/10.1097/SLA.0000000000002347
63. Zhao G, Deng J, Shen Y, Zhang P, Dong H, Xie Z, Xiong L (2019) Hyperhomocysteinemia is key for increased susceptibility to PND in aged mice. Ann Clin Transl Neurol 6(8):1435–1444. https://doi.org/10.1002/acn3.50838
64. Skvarc DR, Berk M, Byrne LK, Dean OM, Dodd S, Lewis M, Marriott A, Moore EM, Morris G, Page RS, Gray L (2018) Post-Operative Cognitive Dysfunction: An exploration of the inflammatory hypothesis and novel therapies. Neurosci Biobehav Rev 84:116–133. https://doi.org/10.1016/j.neubiorev.2017.11.011
65. Nimmerjahn A, Kirchhoff F, Helmchen F (2005) Resting microglial cells are highly dynamic surveillants of brain parenchyma in vivo. Science 308(5726):1314–1318. https://doi.org/10.1126/science.1110647
66. Xu Y, Wang Y, He L, Jiang Z, Huang Z, Liao H, Li J, Saavedra JM, Zhang L, Pang T (2015) Telmisartan prevention of LPS-induced microglia activation involves M2 microglia polarization via CaMKKbeta-dependent AMPK activation. Brain Behav Immun 50:298–313. https://doi.org/10.1016/j.bbi.2015.07.015
67. Qiu LL, Ji MH, Zhang H, Yang JJ, Sun XR, Tang H, Wang J, Liu WX, Yang JJ (2016) NADPH oxidase 2-derived reactive oxygen species in the hippocampus might contribute to microglial activation in

postoperative cognitive dysfunction in aged mice. Brain Behav Immun 51:109–118. https://doi.org/10.1016/j.bbi.2015.08.002

68. Li Y, Pan K, Chen L, Ning JL, Li X, Yang T, Terrando N, Gu J, Tao G (2016) Deferoxamine regulates neuroinflammation and iron homeostasis in a mouse model of postoperative cognitive dysfunction. J Neuroinflammation 13(1):268. https://doi.org/10.1186/s12974-016-0740-2
69. Sun L, Dong R, Xu X, Yang X, Peng M (2017) Activation of cannabinoid receptor type 2 attenuates surgery-induced cognitive impairment in mice through anti-inflammatory activity. J Neuroinflammation 14(1):138. https://doi.org/10.1186/s12974-017-0913-71
70. Ballweg T, White M, Parker M, Casey C, Bo A, Farahbakhsh Z, Kayser A (2021) Association between plasma tau and postoperative delirium incidence and severity: a prospective observational study. Br J Anaesth 126(2):458–466. https://doi.org/10.1016/j.bja.2020.08.061
71. Iovino F, Orihuela CJ, Moorlag HE, Molema G, Bijlsma JJ (2013) Interactions between blood-borne Streptococcus pneumoniae and the blood-brain barrier preceding meningitis. PLoS One 8(7):e68408. https://doi.org/10.1371/journal.pone.0068408
72. Penner MR, Roth TL, Chawla MK, Hoang LT, Roth ED, Lubin FD, Sweatt JD, Worley PF (2011) Age-related changes in Arc transcription and DNA methylation within the hippocampus. Neurobiol Aging 32(12):2198–2210. https://doi.org/10.1016/j.neurobiolaging.2010.01.009
73. Penner MR, Parrish RR, Hoang LT, Roth TL, Lubin FD, Barnes CA (2016) Age-related changes in Egr1 transcription and DNA methylation within the hippocampus. Hippocampus 26(8):1008–1020. https://doi.org/10.1002/hipo.22583
74. Mangold CA, Masser DR, Stanford DR, Bixler GV, Pisupati A, Giles CB, Wren JD, Ford MM (2017) CNS-wide Sexually Dimorphic Induction of the Major Histocompatibility Complex 1 Pathway With Aging. J Gerontol A Biol Sci Med Sci 72(1):16–29. https://doi.org/10.1093/gerona/glv232
75. Oliveira AM (2016) DNA methylation: a permissive mark in memory formation and maintenance. Learn Mem 23(10):587–593. https://doi.org/10.1101/lm.042739.116
76. Rajasethupathy P, Antonov I, Sheridan R, Frey S, Sander C, Tuschl T, Kandel ER (2012) A role for neuronal piRNAs in the epigenetic control of memory-related synaptic plasticity. Cell 149(3):693–707. https://doi.org/10.1016/j.cell.2012.02.057
77. Mohammad F, Pandey GK, Mondal T, Enroth S, Redrup L, Gyllensten U, Kanduri C (2012) Long noncoding RNA-mediated maintenance of DNA methylation and transcriptional gene silencing. Development 139(15):2792–2803. https://doi.org/10.1242/dev.079566
78. Zhang Y, Jurkowska R, Soeroes S, Rajavelu A, Dhayalan A, Bock I, Rathert P, Brandt O (2010) Chromatin methylation activity of Dnmt3a and Dnmt3a/3L is guided by interaction of the ADD domain with the histone H3 tail. Nucleic Acids Res 38(13):4246–4253. https://doi.org/10.1093/nar/gkq147
79. Ooi SK, Qiu C, Bernstein E, Li K, Jia D, Yang Z, Erdjument-Bromage H, Tempst P (2007) DNMT3L connects unmethylated lysine 4 of histone H3 to de novo methylation of DNA. Nature 448(7154):714–717. https://doi.org/10.1038/nature05987

80. Jarome TJ, Butler AA, Nichols JN, Pacheco NL, Lubin FD (2015) NF-kappaB mediates Gadd45beta expression and DNA demethylation in the hippocampus during fear memory formation. Front Mol Neurosci 8:54. https://doi.org/10.3389/fnmol.2015.00054
81. Cho SH, Chen JA, Sayed F, Ward ME, Gao F, Nguyen TA, Krabbe G, Sohn PD (2015) SIRT1 deficiency in microglia contributes to cognitive decline in aging and neurodegeneration via epigenetic regulation of IL-1beta. J Neurosci 35(2):807–818. https://doi.org/10.1523/JNEUROSCI.2939-14.2015
82. Youm YH, Grant RW, McCabe LR, Albarado DC, Nguyen KY, Ravussin A, Pistell P, Newman S (2013) Canonical Nlrp3 inflammasome links systemic low-grade inflammation to functional decline in aging. Cell Metab 18(4):519–532. https://doi.org/10.1016/j.cmet.2013.09.010
83. Murray CA, Lynch MA (1998) Evidence that increased hippocampal expression of the cytokine interleukin-1 beta is a common trigger for age- and stress-induced impairments in long-term potentiation. J Neurosci 18(8):2974–2981. https://doi.org/10.1523/JNEUROSCI.18-08-02974.1998
84. Liu Y, Zhang Y, Fang T, Yang X, Luo X, Guo A, Newell KA (2018) Galantamine improves cognition, hippocampal inflammation, and synaptic plasticity impairments induced by lipopolysaccharide in mice. J Neuroinflammation 15(1):112. https://doi.org/10.1186/s12974-018-1141-5

Figures

Figure 1

Surgery but not anesthesia impaired hippocampus-dependent cognition in aged mice a Experimental design: C57/BL mice (3 m and 18 m) were subjected to laparotomy in a chamber filled with 1.4-2% isoflurane for 20 min. Open field, Y-maze and novel object tests were performed at different time points. b The mice showed a normal total distance traveled in the open field test. c-d The DI of aged mice was decreased in the OLM task but not the ORM task in the 1d group. The spontaneous alternation index (e) and the time spent in the novel arm (f) in the Y-maze test were decreased in aged mice in the 1d group. g-j Simple anesthesia had no effect on the cognitive function of adult and aged mice. n = 9. The data are presented as the mean ± SEM values. **P < 0.01, ***P < 0.001 versus the corresponding group.

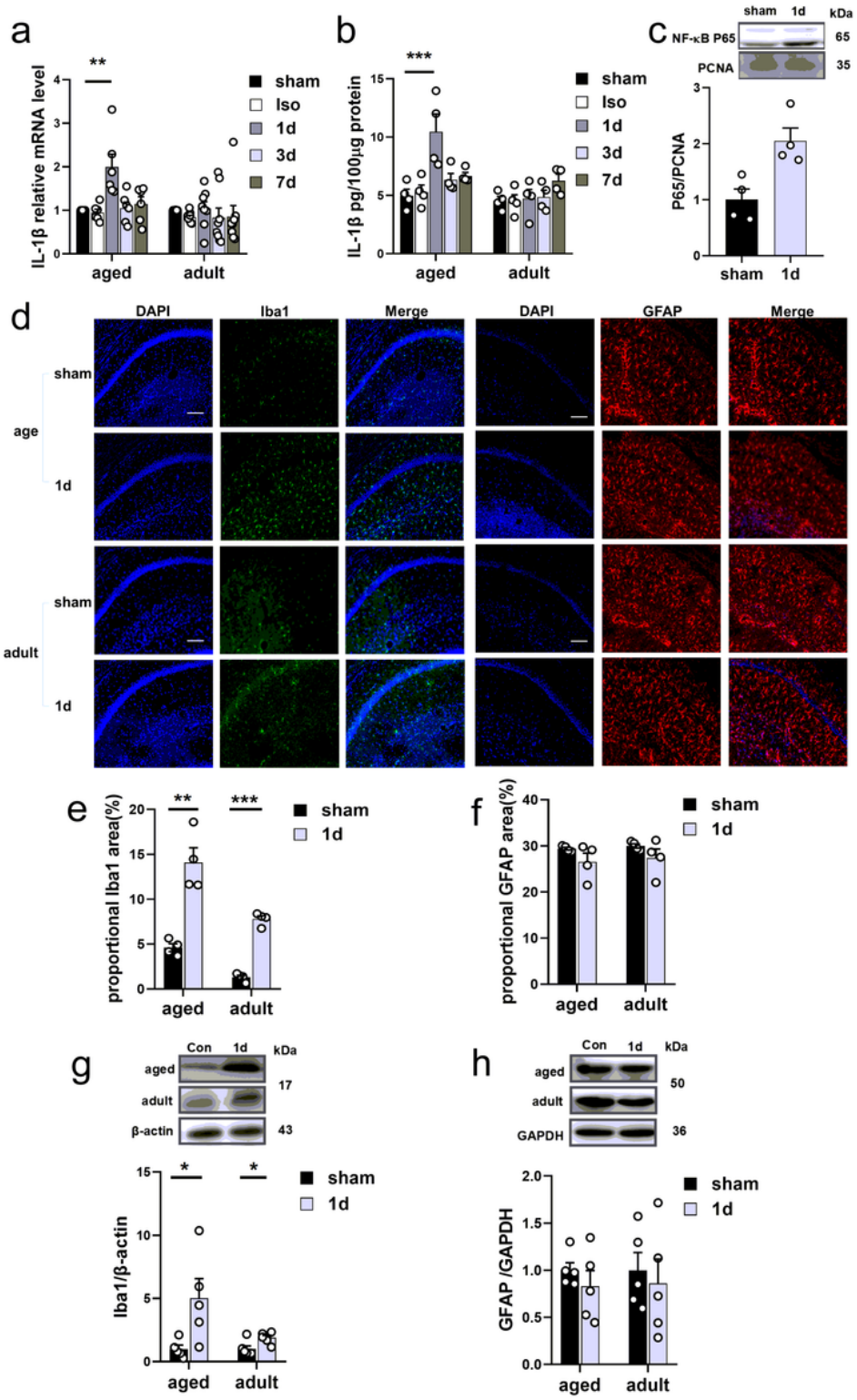

Figure 2

Surgery activated microglia in the dorsal hippocampus a-b The protein and mRNA levels of IL-1β in the dorsal hippocampus were increased in the aged+1d group. c The nuclear expression of NF-κB P65 in the dorsal hippocampus in aged mice was increased 1 day after surgery. d Representative images of Iba1 and GFAP fluorescence in the CA1 region on day 1 after surgery (scale bar = 100 m). e-f Quantification of Iba1 and GFAP fluorescence. g-h The expression of Iba1 was significantly increased in the 1d groups of

aged and adult mice, while GFAP showed no significant difference in the 1d group compared with the sham group. n=4-6. The data are presented as the mean ± SEM values. *P < 0.05, **P < 0.01, ***P < 0.001 versus the corresponding group.

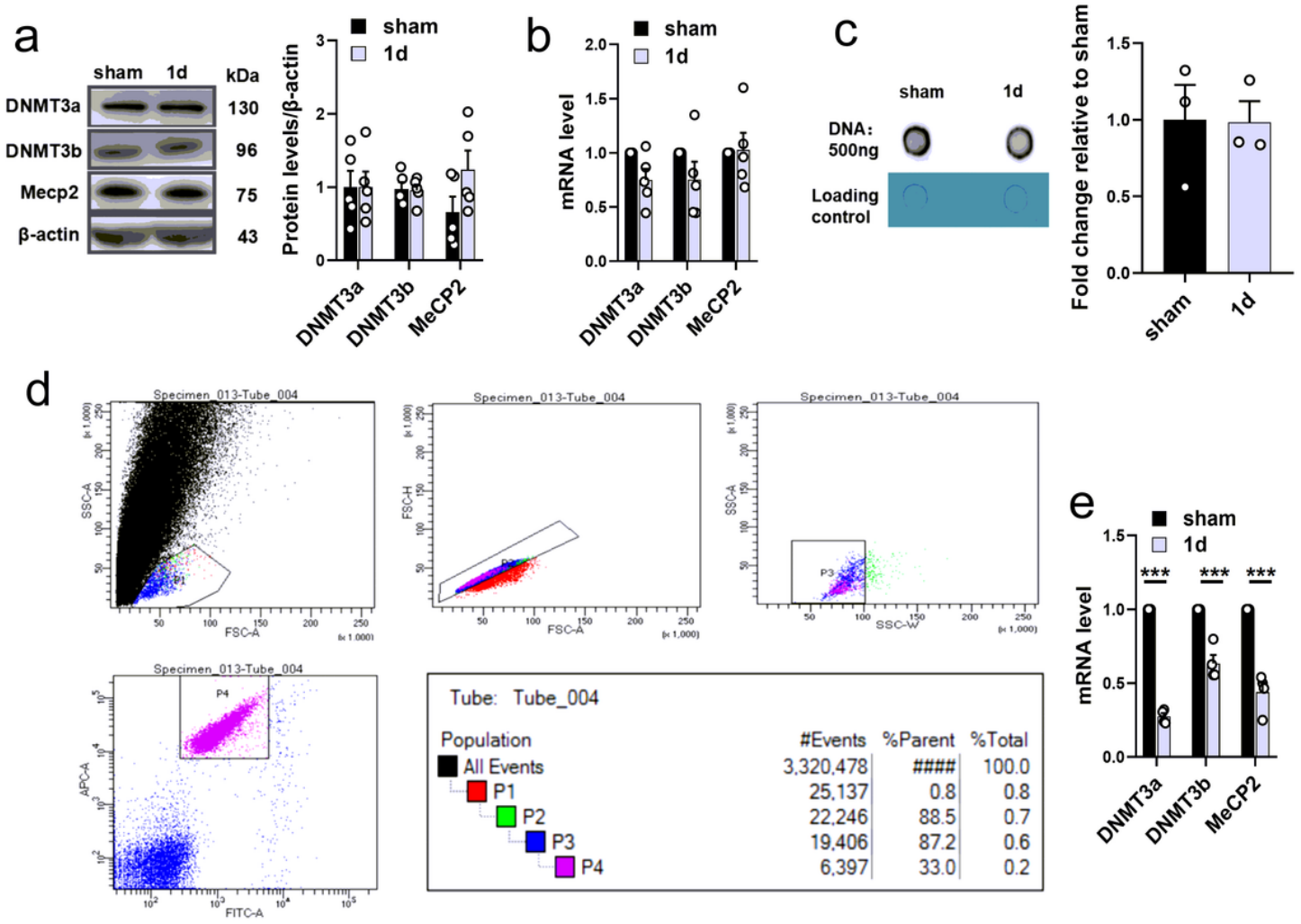

Figure 3

Epigenetic regulators were altered by surgery in sorted microglia but remained unchanged in the dorsal hippocampus a-b The Western blot and RT-PCR results showed no differences in the expression of DNMT3a, DNMT3b, and MeCP2 in the dorsal hippocampus between the 1d group and the sham group of aged mice. c The global 5mC level in the dorsal hippocampus also did not differ between the 1d group and the sham group of aged mice. d Microglia were sorted by flow cytometry from the dorsal hippocampus of aged mice. e The mRNA levels of DNMT3a, DNMT3b and MeCP2 were decreased in sorted microglia from the dorsal hippocampus of aged mice 1 day after surgery. n = 3-5. The data are presented as the mean ± SEM values. ***P < 0.001 versus the corresponding group.

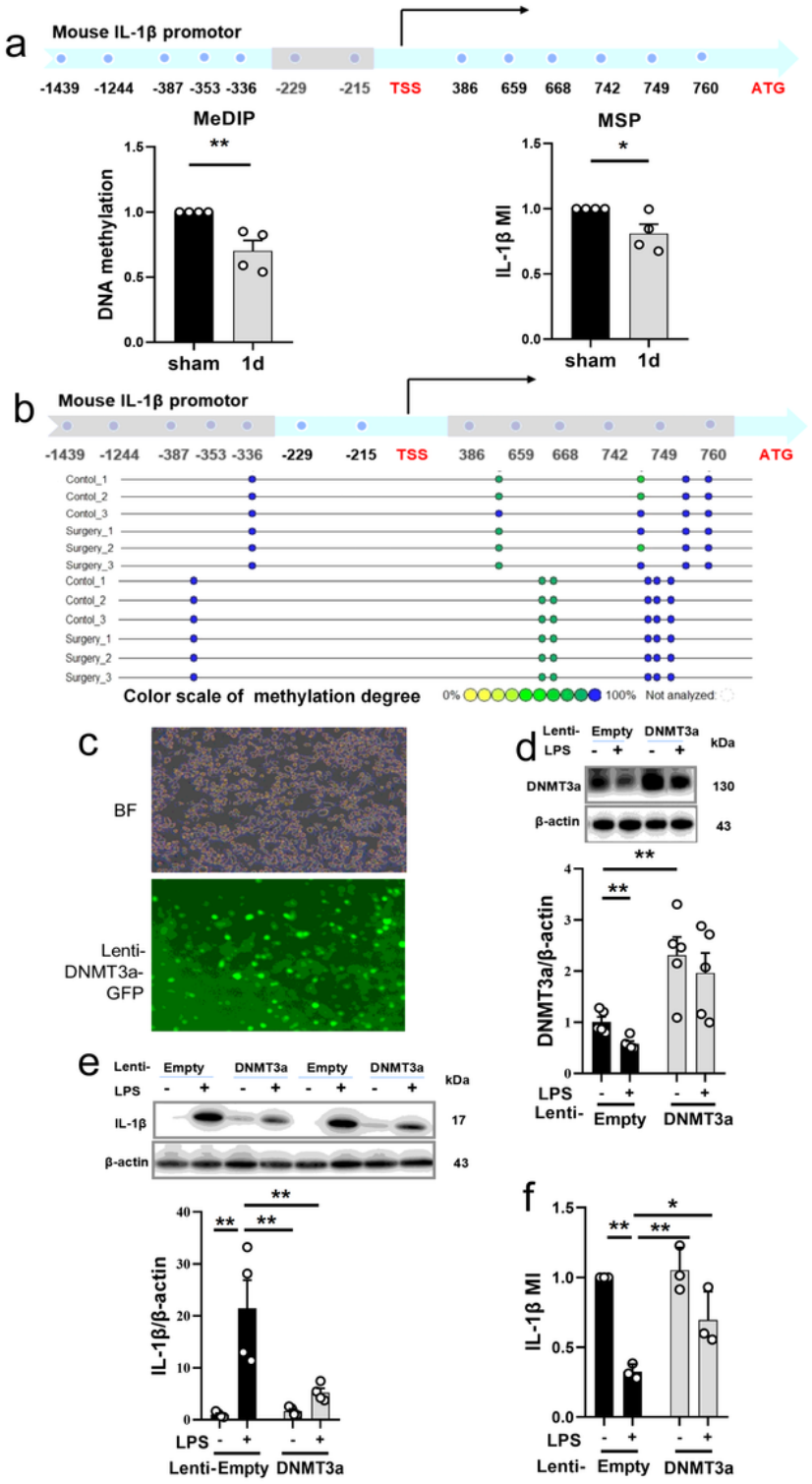

Figure 4

Surgery decreased DNA methylation of IL-1β promoter in aged mice a The MeDIP and MSP results showed that the DNA methylation level in the IL-1β promoter region in aged mice was significantly decreased 1 day after surgery at the -215 bp and -229 bp sites. b However, into decreases were not observed at the other CpG sites in IL-1β. c BV2 cells were effectively transduced with Lenti-GFP. d-f Overexpression of DNMT3a in BV2 cells reversed the LPS-induced increase in IL-1β expression and

decrease in the IL-1β promoter DNA methylation level. n = 3-5. The data are presented as the mean ± SEM values. *P < 0.05, **P < 0.01 versus the corresponding group.

Figure 5

IL-1β impaired synaptic plasticity after surgery in aged mice a Experimental design. b A single administration of IL-1ra prevented the surgery-induced increase in IL-1β expression in aged mice 1 day after surgery. c-d IL-1ra reversed the decrease in dendritic spine density in the dorsal hippocampus of aged mice one day after surgery. (Scale bar = 5 m). e-h IL-1ra reversed the decreases in the expression of PSD95, Syn, and BDNF in the dorsal hippocampus of aged mice one day after surgery. i Surgery reduced the number of c-Fos+ neurons in the dorsal hippocampus of aged mice, and IL-1ra reversed this effect. n = 4-5. The data are presented as the mean ± SEM values. *P < 0.05, ***P < 0.001 versus the corresponding group.

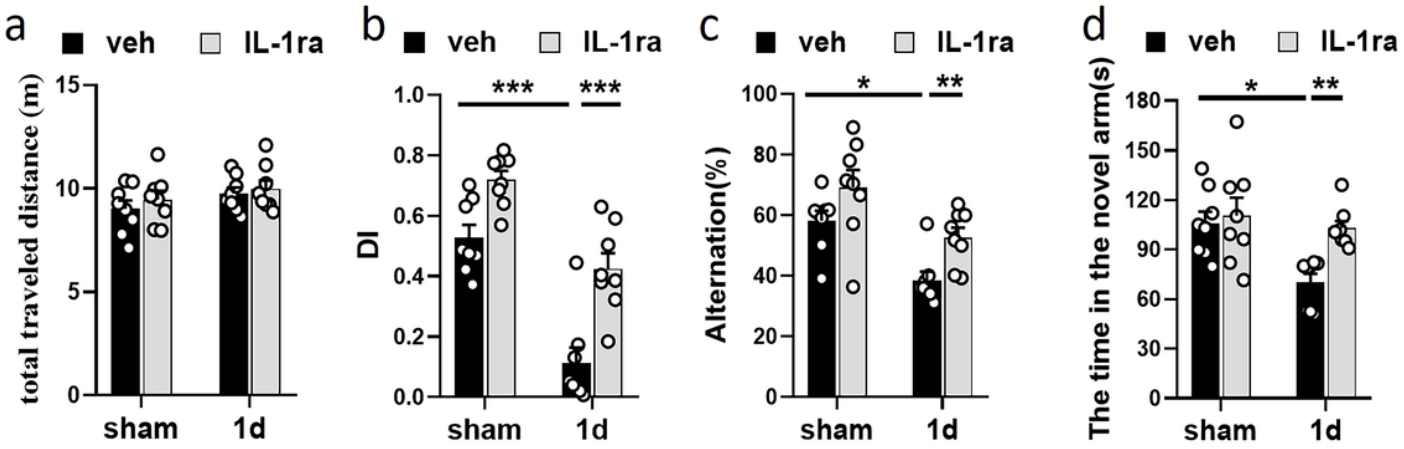

Figure 6

Inhibiting IL-1β in the dorsal hippocampus rescued memory deficits induced by surgery a The mice showed a normal total distance traveled in the open field test. b-d The reductions in the DI, spontaneous alternation index, and time spent in the novel arm were reversed in aged mice by inhibiting IL-1β via administration of IL-1ra. n = 8. The data are presented as the mean ± SEM values. *P < 0.05, **P < 0.01, ***P < 0.001 versus the corresponding group.

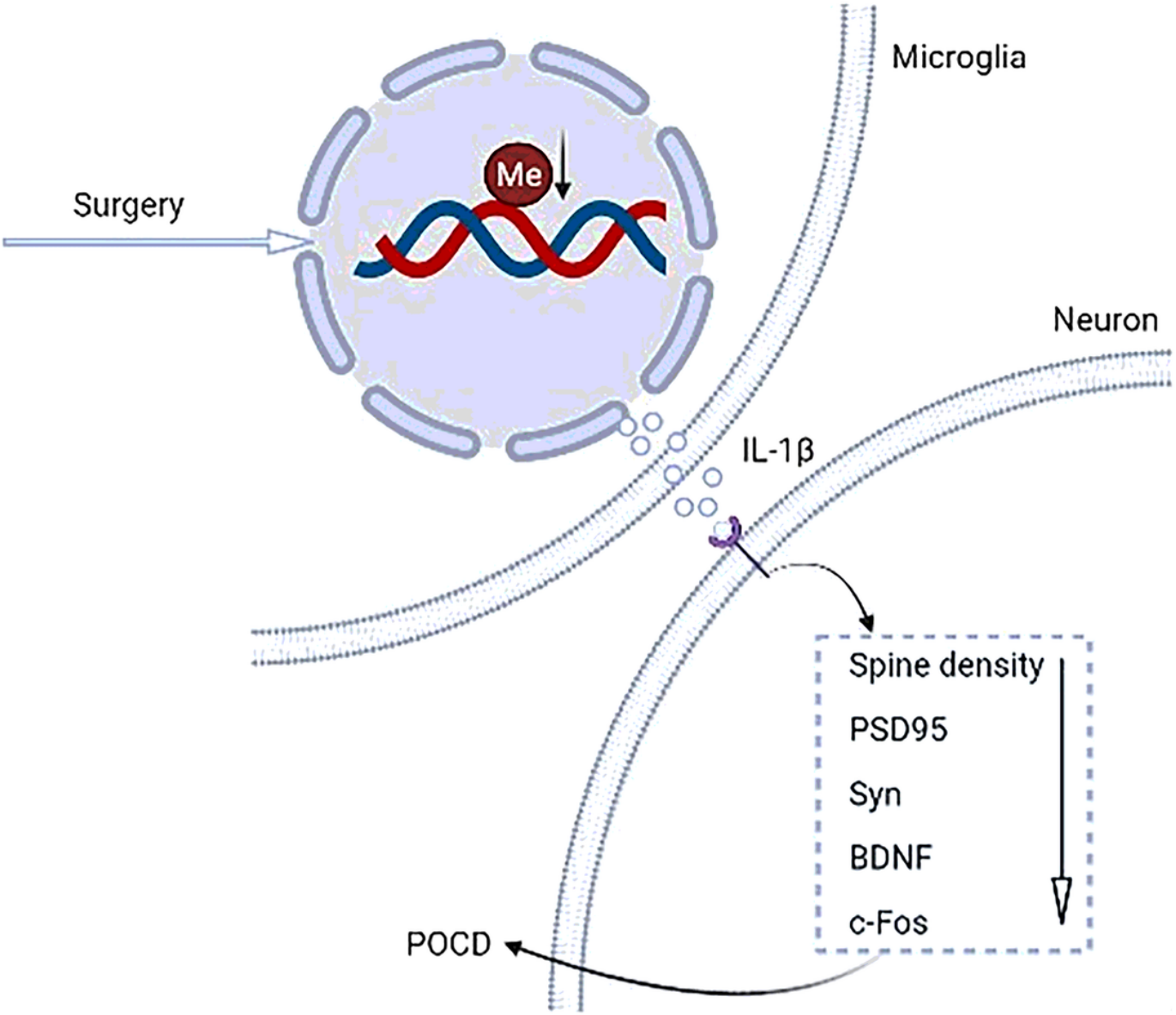

Figure 7

Schematic representation of the roles of IL-1β and DNA methylation in surgery-associated learning and memory deficits in aged mice

Supplementary Files

This is a list of supplementary files associated with this preprint. Click to download.

- SI.pdf